Vol. **2**, **6**. 629-640 (2013)

Revue de Mécanique Appliquée et Théorique

Assessment of chip segmentation process in machining using physical parameters

S. ATLATI

Université de Lorraine, Laboratoire d'Énergétique et de Mécanique Théorique et Appliquée (LEMTA) CNRS-UMR 7563, GIP-InSIC, 27 rue d'Hellieule, F-88100, Saint Dié des Vosges-France

Université Mohamed I, Equipe de Mécanique et Calcul Scientifique (EMCS), ENSAO, Oujda-Morocco.

B. HADDAG

Université de Lorraine, Laboratoire d'Énergétique et de Mécanique Théorique et Appliquée (LEMTA) CNRS-UMR 7563, GIP-InSIC, 27 rue d'Hellieule, F-88100, Saint Dié des Vosges-France

M. NOUARI

Université de Lorraine, Laboratoire d'Énergétique et de Mécanique Théorique et Appliquée (LEMTA) CNRS-UMR 7563, GIP-InSIC, 27 rue d'Hellieule, F-88100, Saint Dié des Vosges-France

M. ZENASNI

Université Mohamed I, Equipe de Mécanique et Calcul Scientifique (EMCS), ENSAO, Oujda-Morocco.

Abstract

The chip segmentation process has a significant effect on the cutting force fluctuation during machining which could affect tool vibration and tool wear. This paper deals with a quantitative analysis of the chip segmentation phenomenon in metal cutting. The notion of intensity of the phenomenon has been introduced. Various parameters have been proposed for this purpose. These parameters are based on dimensional characteristics of the segmented chip and the strain distribution within the chip. A Finite Element based modelling has been developed to simulate the chip formation process in the case of machining aeronautical aluminium alloy AA2024-T351 with WC-Co based cutting tools. From the simulated chip morphologies, introduced chip segmentation parameters are assessed. The impact of the cutting speed and tool geometry on the chip segmentation intensity is clearly highlighted. Cutting force and contact length fluctuations with respect to the cutting speed variation when segmentation occurs are discussed and deeply analysed. A correlation between speed increases as well as between chip formation process and average cutting force oscillation has been established thanks to the introduced parameters, showing thus their usefulness.

Keywords: Metal machining; Chip morphology; Segmentation intensity; FE modelling

Résumé

Le processus de la segmentation du copeau a un effet significatif sur la fluctuation de l'effort de coupe lors de l'usinage qui peut affecter les vibrations et l'usure de l'outil. Cet article traite l'analyse quantitative du phénomène de la segmentation du copeau pour la coupe des métaux. La notion d'intensité du phénomène a été introduite. Différents paramètres ont été proposés. Ces paramètres sont basés sur les caractéristiques dimensionnelles du

copeau segmenté et la distribution de la déformation plastique à l'intérieure du copeau. Une modélisation basée sur la Méthode des Eléments Finis « MEF » a été développée afin de simuler le processus de la formation des copeaux pendant l'usinage de l'alliage d'aluminium aéronautique AA2024-T351 avec des outils de WC-Co. A partir des morphologies des copeaux simulés, les paramètres introduits de la segmentation des copeaux sont évalués. L'impact de la vitesse de coupe et de la géométrie de l'outil sur l'intensité de la segmentation des copeaux est clairement mis en évidence. L'effort de coupe et la fluctuation de la longueur de contact en fonction de la vitesse de coupe quand la segmentation a eu lieu sont analysés. Une corrélation entre la vitesse moyenne et le processus de la formation des copeaux d'une part et l'oscillation des efforts de coupe d'autre part a été établie grâce aux paramètres introduits, ce qui montre leur utilité.

Mot clés: Usinage des matériaux métalliques; Morphologie des copeaux; Intensité de segmentation; Modélisation élément finis

Nomenclature

Cutting parameters

V_c	Cutting speed [m/min]
f	Feed [mm]
α , γ	Tool-rake and clearance angles [°]
F_c	Cutting force [N]

Chip morphology parameters

$h_{\min}$	Minimum chip thickness
$h_{\max}$	Maximum chip thickness
h_{mean}	Average chip thickness
h_0	Uncut chip thickness, equal feed
CR	Chip compression ratio
$CR_{\min}$	Minimum chip compression ratio
$CR_{\max}$	Maximum chip compression ratio
CR_{mean}	Average chip compression ratio
l_s	Chip segmentation length
f_s	Chip segmentation frequency
SR_{ref}	Reference chip segmentation ratio
$SR_{\min}$	Minimum chip segmentation ratio
$SR_{\max}$	Maximum chip segmentation ratio
SR_{mean}	Average chip segmentation ratio
SIR	Chip segmentation intensity ratio

Mechanical quantities

$\boldsymbol{\sigma}$	True or Cauchy stress tensor [MPa]
$\tilde{\boldsymbol{\sigma}}$	Effective stress tensor (not affected by damage)
ρ	Material density [kg/m^3]

E , ν	Young modulus [GPa] and Poisson's ratio
A , B , C , m , n	Workmaterial parameters in Johnson-Cook flow stress law
$\bar{\varepsilon}^p$	Von Mises equivalent plastic strain
$\dot{\bar{\varepsilon}}^p$	Von Mises equivalent plastic strain-rate
$\dot{\bar{\varepsilon}}_0$	Reference equivalent plastic strain-rate
$\bar{\sigma}$	Von Mises equivalent stress [MPa]
ω_d	Damage initiation criterion
d	Damage variable
G_f	Fracture strain energy
σ_n	Normal friction stress [MPa]
τ_f	Shear friction stress [MPa]
μ	Friction coefficient
$\tau_{\max}$	Shear stress limit [MPa]
V_s	Sliding velocity at the tool-workpiece interface [m/s]

Thermal quantities

T	Temperature [°C]
T_0	Reference ambient temperature [°C]
T_m	Melting temperature [°C]
λ	Thermal conductivity [W/m/°C]
c_p	Specific heat capacity [J/kg/°C]
α	Thermal expansion [µm/m/°C]
η_p	Plastic work conversion factor (Taylor-Quinney factor)
η_f	Frictional work conversion factor
f_f	Fraction of the friction energy conducted into the tool (heat partition coefficient)
h	Heat transfer coefficient for the tool-workpiece interface [kW/m^2/°C]
$\dot{q}_p$	Volumetric heat generation due to plastic work [W/m^3]
$\dot{q}_f$	Volumetric heat generation due to friction work [W/m^3].

1. INTRODUCTION

In metal cutting, the chip morphology is an important indicator of the cutting process stability. This morphology depends on several parameters, which can be classified on cutting parameters (cutting speed, feed rate, and depth of cut), cutting configuration (tool geometry and cutting angles), and tool workmaterial couple behaviour (thermomechanical loading and contact with friction). According to these parameters, continuous, segmented, serrated or fragmented chips can be obtained, as classified by Komanduri and Brown [1]. Many research works have been conducted on different machining

processes to highlight the impact of cutting conditions on the chip formation process ([1]-[3]). One of the most studied phenomena in machining is the chip segmentation, corresponding to the development of the so-called adiabatic shear bands giving rise to particular chip morphology, oscillation of cutting forces, roughness variation of the machined surface a well as fluctuation of the tool–workpiece contact. In this study, several parameters are proposed to quantify the chip morphology, especially the chip segmentation phenomenon. The notion of intensity of the phenomenon has been introduced. In the first section global chip morphology and chip segmentation parameters are listed. The first set of proposed parameters are variants of the well-known chip compression ratio, these second set is variants of chip segmentation parameters proposed here to assess the relative variation of the chip thickness, and the last one is a parameter that enables to quantify the chip segmentation intensity using the relative variation of the local strain in the segmented chip. To assess all these parameters, machining the aeronautical aluminium alloy AA2024-T351 with cemented tungsten carbide (WC-Co) cutting tools under an orthogonal cutting configuration has been considered as a sample application, but the proposed parameters can be used for analysis of other tool–workpiece couples. To highlight the impact of cutting conditions on the chip morphology, a FE model representing the cutting tests has been developed. A correlation between the formed chip segment and the instantaneous cutting force has been discussed.

2. CHIP MORPHOLOGY AND CHIP SEGMENTATION PARAMETERS

Analysis of the chip morphology allows understanding the cutting process and also gives information about the adequate conditions to be used for a stable cutting process. As shown by Fig. 1, usually the chip morphology is quantified by the classical parameter, known as the chip compression ratio (*CR*), which is given by:

$$CR = \frac{h}{f} \tag{1}$$

where h and f are deformed and undeformed chip thickness respectively. This parameter is a first approximation of the total strain occurred in the chip. Astakov et al. [4] and Astakov [5] use extensively this parameter to highlight the impact of cutting parameters on the cutting process and suggest the weighting method [4] to estimate it experimentally for some machining processes. However when the chip shows fluctuations of its thickness, as shown in Fig. 1, the question about assessing this parameter a rises, because the value of h is variable. A simple way to evaluate it in such case (segmented chips) consists to define maximum, average quantities, as follows:

$$\begin{aligned} CR_{\min} &= \frac{h_{\min}}{f} \\ CR_{\max} &= \frac{h_{\max}}{f} \\ CR_{mean} &= \frac{\frac{1}{2}\left(h_{\min} + h_{\max}\right)}{f} = \frac{1}{2}\left(CR_{\min} + CR_{\max}\right) \end{aligned} \tag{2}$$

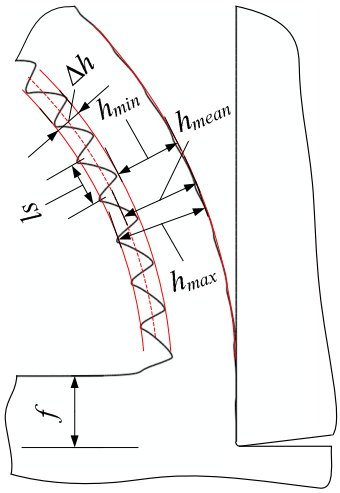

Fig. 1. Geometric parameters for the assessment of chip compression ratios, segmentation length and chip segmentation ratios.

In order to quantify the chip segmentation phenomenon, classical parameters are usually used, which are the chip segmentation frequency and the chip segmentation length. These two parameters are related by the following relationship:

$$f_s = \frac{V_c}{l_s} \tag{3}$$

Parameters f_s and l_s are only indicators of the apparition of successive shear localization bands in the chip, but they did not give information about the intensity of the phenomenon, which allows more understanding of the impact of cutting conditions on the cutting process. So from a scientific point of view other adequate parameters have to be defined. Using the maximum and minimum chip thicknesses ($h_{\max}$ and $h_{\min}$), the following parameters are defined to quantify the chip segmentation:

$$\begin{aligned} SR_{ref} &= \frac{\Delta h}{f} = \frac{h_{\max} - h_{\min}}{f} \\ SR_{\min} &= \frac{\Delta h}{h_{\max}} = 1 - \frac{h_{\min}}{h_{\max}} \\ SR_{\max} &= \frac{\Delta h}{h_{\min}} = \frac{h_{\max}}{h_{\min}} - 1 \\ SR_{\text{mean}} &= \frac{\Delta h}{h_{mean}} = 2\frac{h_{\max} - h_{\min}}{h_{\max} + h_{\min}} \end{aligned} \tag{4}$$

These parameters can be shown as a global measure of the shear strain in a chip segment and can be evaluated easily from the different chip thicknesses, i.e. undeformed chip thickness, maximum chip thickness $h_{\max}$ and minimum chip thickness $h_{\min}$. In order to take into account more of the local strain within the chip when segmentation occurs, a new parameter, called Segmentation Intensity Ratio, is introduced. The *SIR* parameter is defined as a ratio between the equivalent plastic strain inside the shear bands and the equivalent plastic strain outside the shear bands, i.e. between successive adiabatic shear bands, [6]:

$$SIR = \frac{\bar{\varepsilon}_{in}^{p}}{\bar{\varepsilon}_{out}^{p}} \tag{5}$$

Using this parameter, the impact of cutting conditions as well as tool geometry on the chip segmentation intensity can be highlighted. In practice, to evaluate the *SIR* parameter, the equivalent plastic strain inside shear bands, $\bar{\varepsilon}_{in}^{p}$, and outside bands, $\bar{\varepsilon}_{out}^{p}$, should be calculated.

3. MODELLING OF THE CUTTING PROCESS

3.1 WORKMATERIAL BEHAVIOUR

To reproduce chip segmentation phenomenon, specifically localized shear bands, different strategies are used in the frame of finite element modelling. In some previous works, damage is considered in the constitutive model of the workpiece material (e.g. [7]-[8]). In other works, an adequate strain softening modelling is considered, without any damage modelling (e.g. [9]-[10]). In the present work, the first strategy is adopted.

To represent the behaviour of the workpiece material during machining, a Johnson-Cook thermo-visco-plastic-damage model has been adopted, as developed in [11]. Fig.2 gives a schematic representation of plastic strain, plastic strain-rate, temperature and damage effects on the stress-strain behaviour of a ductile metal. The main equations of the model are given below.

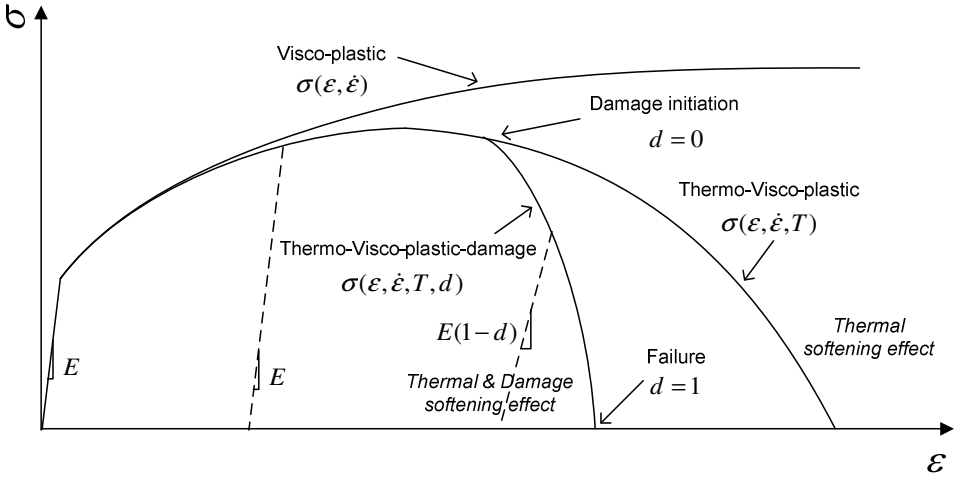

Fig. 2. Schematic representation of plastic strain, plastic strain-rate, temperature and damage effects on the stress-strain behaviour of a ductile metal.

The flow stress is given by Johnson-Cook law [12]:

$$\bar{\sigma} = \underbrace{\left[A + B(\bar{\varepsilon}^{p})^{n}\right]}_{\text{Hardening}} \underbrace{\left[1 + C \ln \dot{\bar{\varepsilon}}^{*}\right]}_{\text{Viscosity}} \underbrace{\left[1 - T^{*m}\right]}_{\text{Softening}} \tag{6}$$

$$\text{with} \quad \dot{\bar{\varepsilon}}^{*} = \frac{\dot{\bar{\varepsilon}}^{p}}{\dot{\bar{\varepsilon}}_{0}} \quad \text{and} \quad T^{*} = \frac{T - T_{0}}{T_{m} - T_{0}}$$

where *A*, *B*, *C*, *m* and *n* are the material parameters, $\bar{\varepsilon}^p$ the von Mises equivalent plastic strain, $\dot{\bar{\varepsilon}}^p$ the von Mises equivalent plastic strain rate, $\dot{\bar{\varepsilon}}_0$ the reference equivalent plastic strain rate, T_m and T_0 are, respectively, the material melting temperature and the reference ambient temperature.
The fracture behaviour is described by a damage initiation criterion and a damage evolution law up to fracture. The damage initiation criterion is given by the following relationship:

$$\omega_d = \int \frac{d\bar{\varepsilon}^p}{\bar{\varepsilon}_d^p} \quad \text{with} \quad 0 \le \omega_d \le 1$$

$$\bar{\varepsilon}_d^p = \underbrace{\left[d_1 + d_2 e^{\left(d_3 \frac{P}{\bar{\sigma}} \right)} \right]}_{\text{Stress triaxiality}} \underbrace{\left[1 + d_4 \ln \dot{\bar{\varepsilon}}^* \right]}_{\text{Viscosity}} \underbrace{\left[1 - d_5 T^* \right]}_{\text{Température}} \tag{7}$$

where $\bar{\varepsilon}_d^p$ the equivalent plastic strain at the onset of damage, function of the stress triaxiality factor $P / \bar{\sigma} = -\frac{1}{3} Tr(\boldsymbol{\sigma}) / \sqrt{\frac{3}{2} \boldsymbol{\sigma} : \boldsymbol{\sigma}}$, equivalent plastic strain rate and temperature, while $d_1 - d_5$ are the material damage parameters. The criterion for damage initiation is met when $\omega_d = 1$.
The damage evolution can be expressed by the following relationships:

$$d = \begin{cases} \dfrac{\bar{u}^p}{\bar{u}_f} = \dfrac{L\,\bar{\varepsilon}^p}{\bar{u}_f} = \dfrac{2 G_f L\,\bar{\varepsilon}^p}{\bar{\sigma}} & \text{linear evolution} \\ 1 - exp\left(-\displaystyle\int_0^{\bar{u}^p} \frac{\bar{\sigma}}{G_f} d\bar{u}^p \right) & \text{exponential evolution} \end{cases} \tag{8}$$

where $\bar{u}^p$ is the equivalent plastic displacement, function of the equivalent plastic strain $\bar{\varepsilon}^p$ and the characteristic length L of the corresponding finite element, while $\bar{u}_f$ is the equivalent plastic displacement at failure, and G_f is the fracture strain energy, related to stress intensity factors as follow:

$$\left(G_f \right)_{I,II} = \left((1 - \nu)^2 / E \right) \left(K_C^2 \right)_{I,II} \tag{9}$$

where K_C is the fracture toughness (characteristic of the material)) and subscript *I*, *II* refer to opening and shearing modes, respectively [13].
Damage evolution laws, as given by Eq. (8), are proposed in the context of Finite Element method to reduce the mesh dependency effect at strain localisation.
The true stress tensor is defined as:

$$\boldsymbol{\sigma} = (1 - d)\, \tilde{\boldsymbol{\sigma}} \tag{10}$$

where $\tilde{\boldsymbol{\sigma}}$ is the effective stress, representing stress state that would exist in the material if no damage occurs [14].
As the mechanical behaviour is affected by temperature, the mechanical plastic work generates heat flux which result in temperature rise. The heat flux due to this phenomenon is described the following relation:

$$\dot{q}_p = \eta_p \bar{\sigma} : \dot{\bar{\varepsilon}}^p \tag{11}$$

Where η_p is the plastic work conversion factor, generally taken equal to 0.9 for metals. In this work, the same value is used for the plastic work conversion factor.

3.2 TOOL–WORKPIECE INTERFACE BEHAVIOUR

The contact behaviour at the tool-workpiece interface is defined by the relationship between the normal friction stress σ_n and the shear friction stress τ_f, as follow:

$$\tau_f = \begin{cases} \mu\sigma_n & \text{if} \quad \mu\sigma_n < \tau_{\max} \\ \tau_{\max} & \text{if} \quad \mu\sigma_n \geq \tau_{\max} \end{cases} \tag{12}$$

where μ is the friction coefficient and $\tau_{\max}$ is the shear stress limit considered equal to the initial plastic flow shear stress.
The friction at the contact interface may generate a heat flux which is evaluated by the following relation:

$$\dot{q}_f = f_f \eta_f \tau_f V_s \tag{13}$$

with $\dot{\gamma}$ is the slip rate, τ_f the friction stress given by Eq.(12), η_f the frictional work conversion factor, and f_f the fraction of the thermal energy conducted into the chip. By assuming all the frictional work converted into heat, $\eta_f = 1$ is often considered and also used in this work. The value of f_f depends on the thermal properties of the cutting tool and workpiece material as well as the temperature gradient near the chip-tool interface, [15]. Here, f_f is taken constant.
As indicated before, a part of the mechanical inelastic work transforms to heat, so a part of the heat flux $\dot{q}$ is a function of the flow stress and the plastic strain (see Eq.(11)). In addition, at the contact interface zone a part of $\dot{q}$ is generated by friction (see Eq.(13)), so the heat flux in the thermal equilibrium equation can be written as $\dot{q} = \dot{q}_p + \dot{q}_f$.

3.3 FINITE ELEMENT MODEL

To analyse the impact of cutting conditions on chip formation process, mainly on the chip segmentation, a two-dimensional FE model for orthogonal cutting tests, has been developed in Abaqus/Explicit software, as shown in Fig. 3. Cutting speed, feed and rake angle are variables. To

generate the chip, a thin layer is defined in the workpiece, with thickness $dl = 20\mu m$, to be deleted as the cutting tool advances in the workmaterial. In the chip layer, with thickness equal the feed, as well as in the deleted layer a thermo-viscoplastic-damage behaviour is used, while in the zone below the machined surface, a thermo-viscoplastic behaviour is adopted. The cutting tool is considered rigid with thermal behaviour.

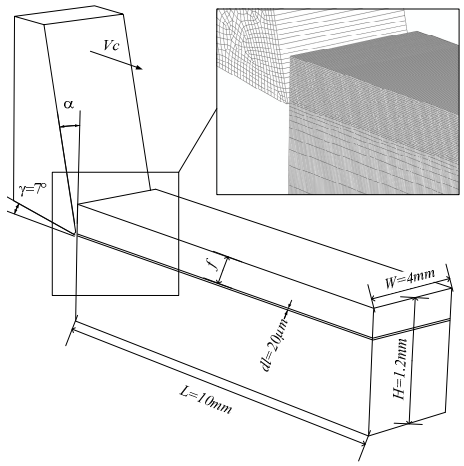

Fig. 3. FE model used for the orthogonal cutting simulation tests

4. RESULTS AND DISCUSSIONS

4.1 ASSESSMENT OF THE CHIP SEGMENTATION INTENSITY RATIO

The intensity of chip segmentation phenomenon can be also quantified using the last parameter introduced in Section 2, i.e. the chip segmentation intensity ratio, given by Eq.(5). This parameter involves local strain in and out of shear bands within the segmented chip. To quantify the relative variation of the strain in the chip, i.e. "*SIR"*, the proposed method consists to define a path along the mid-thickness of the chip, as shown in Fig. 4, and then the equivalent plastic stain is plotted along this path. Then, equivalent plastic strains are taken as average values of maximum and minimum peaks of the plastic strain curve, respectively. The "*SIR"* parameter is computed as follows. The Fig. 5 shows the effect of cutting conditions (rake angle and cutting speed) on Segmentation intensity ratio "SIR" for fixed feed.

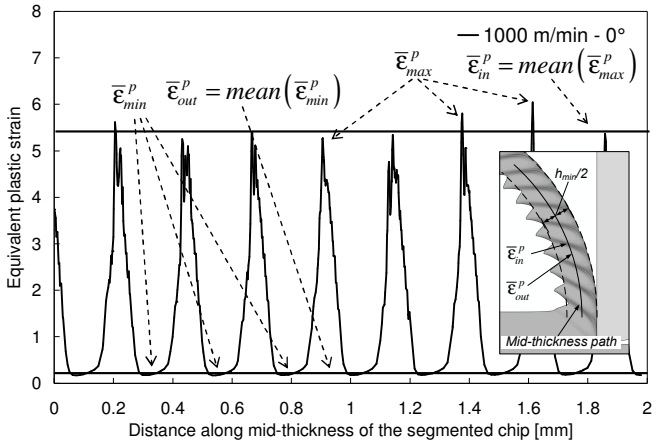

Fig. 4. Illustration of the assessment of average values of $\overline{\varepsilon}^p_{in}$ and $\overline{\varepsilon}^p_{out}$ in the frame of FEM

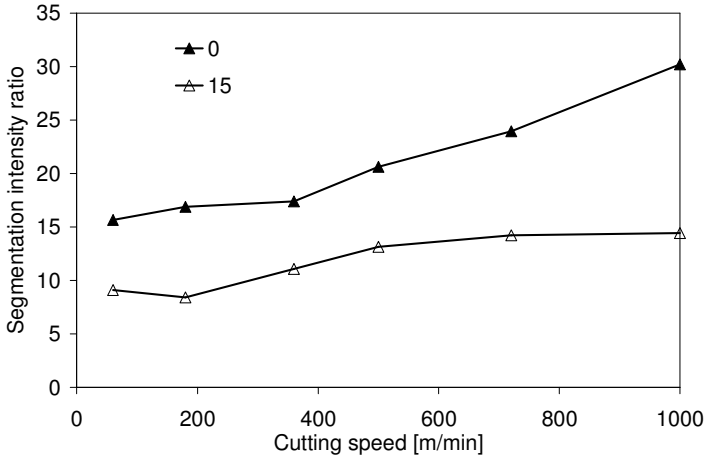

Fig. 5. Segmentation intensity ratio as function of cutting speed, for two rake angles (0°, 15°) and fixed feed (0.3mm).

For the same tool geometry (one rake angle), segmentation intensity is nonlinearly proportional to the cutting speed. So, by increasing cutting speed at high strain localization in shear bands will occur. Three domains can then be distinguished with respect to the cutting speed evolution. At low cutting speed, there is basically no change in the chip segmentation intensity. At moderate cutting speeds, the value of the "*SIR"* parameter increases rapidly and at high cutting speed, a quasi-stagnation of "*SIR"* is observed for rake angle of 15°, while for rake angle of 0°, it continues to increase. The extreme case (high cutting speed and small rake angle) gives rise to large "*SIR"* values, so chip fragmentation may occur. Hence, it is possible to control completely the chip segmentation by acting simply on the rake angle and/or cutting speed. The combined effect of these cutting parameters enables to control the cutting process by promoting the chip fragmentation, via the increase of the chip segmentation intensity.

4.2 CORRELATION BETWEEN CHIP SEGMENTATION AND CUTTING FORCE

A close correlation can be established between chip segmentation intensity and average cutting force, using "*SIR*" Fig. 6 (a) and SR_{ref} Fig. 6 (b) parameters. As shown in Fig. 6, for each tool geometry when cutting speed increases average cutting force decreases and "*SIR*" and SR_{ref} parameters increase. This confirms the fact that the chip segmentation phenomenon is the origin of the cutting force reduction for the machined material considered here.

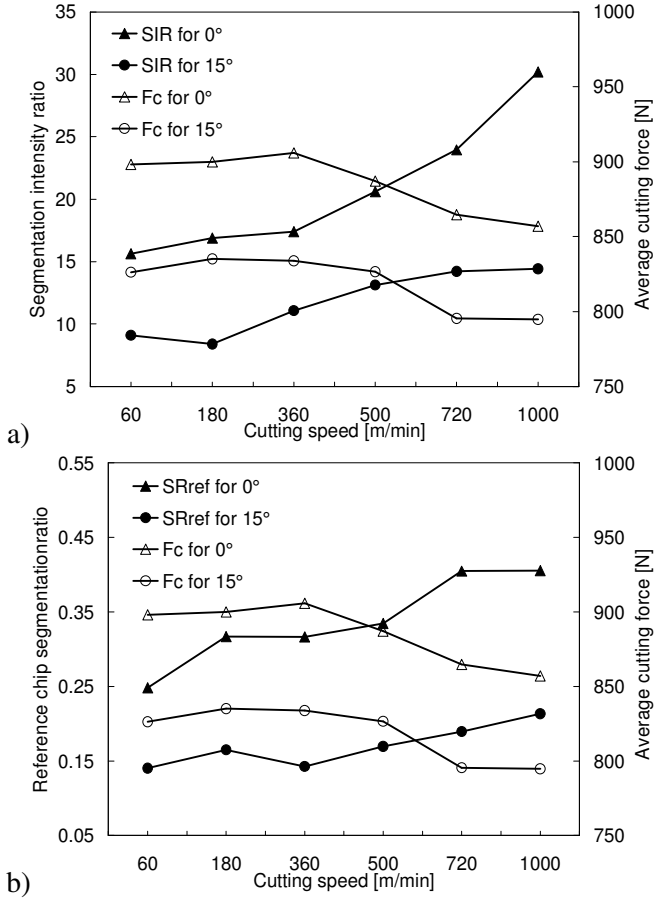

Fig. 6. Correlation between average cutting force, (a) segmentation intensity ratio, and (b) reference chip segmentation ratio

5. CONCLUSION

Analysis of the chip morphology, especially the chip segmentation phenomenon, has been performed in the present study. Machining under orthogonal cutting configuration of the usual aluminium alloy AA2024-T351 with two rake angles cemented carbide tools WC-Co have been considered. Several parameters have been introduced to quantify the chip segmentation phenomenon. The notion of intensity of the phenomenon has been introduced. It has been shown that chip segmentation length and chip segmentation frequency parameters are not sufficient to quantify the chip segmentation phenomenon, since segmentation length is quasi-independent of the cutting speed, while segmentation frequency is proportional to the cutting speed. However the impact of the rake angle has been

highlighted using these two parameters. Introduced chip segmentation parameters showed that all chip segmentation ratios increase nonlinearly with cutting speed.

6. REFERENCES

1. Komanduri R., Brown. R. H, On the mechanics of chip segmentation in machining, Journal of Engineering for Industry 103 (1981) 33–51.

2. Barry J., Byrne G., The mechanisms of chip formation in machining hardened steels, Journal of Manufacturing Science and Engineering 124 (2002) 528–535.

3. Komanduri R., Turkovich B. F., New observations on the mechanism of chip formation when machining titanium alloys, Wear 69 (1981) 179–188.

4. Astakhov V. P., Shvets S., The assessment of plastic deformation in metal cutting, Journal of Materials Processing Technology 146 (2004) 193–202.

5. Astakhov V. P., Tribology of Metal Cutting, Elsevier, London, 2006 (Edition).

6. Atlati S., Haddag B., Nouari M., Znasni M., Analysis of a new Segmentation Intensity Ratio ‘‘SIR’’ to characterize the chip segmentation process in machining ductile metals, International Journal of Machine Tools and Manufacture 51 (2011) 687–700.

7. Guo Y.B., Yen D.W., A FEM study on mechanisms of discontinuous chip formation in hard machining, Journal of Materials Processing Technology 155–156 (2004) 1350–1356

8. Lin Z.C., Lin Y.Y., Three-dimensional elastic-plastic finite element analysis for orthogonal cutting with discontinuous chip of 6-4 brass, Theoretical and Applied Fracture Mechanics 35 (2001) 137-153.

9. Aurich J.C., Bil H., 3D Finite Element Modelling of Segmented Chip Formation, CIRP Annals – Manufacturing Technology 52 (1) (2006) 47–50.

10. Ohbuchi Y., Obikawa T., Adiabatic shear in chip formation with negative rake angle, International Journal of Mechanical Sciences 47 (2005) 1377-1392.

11. Abaqus/Explicit, Documentation for version 6.8, 2008, Dassault Systems Simulia.

12. Johnson G. R., Cook W. H., Fracture characteristics of three metals subjected to various strains, strain rates, temperatures and pressures, Engineering Fracture Mechanics 21 (1985) 31–48.

13. Mabrouki T., Girardin F., Asad M., Rigal J.-F., Numerical and experimental study of dry cutting for an aeronautic aluminium alloy (A2024-T351), International Journal of Machine Tools and Manufacture 48 (2008) 1187-1197.

14. Lemaitre J., Chaboche J.L., Mécanique des matériaux solides. Edition Dunod, Paris (1985).

15. Komanduri R., Hou Z.B., Thermal modelling of the metal cutting process - Part II: temperature rise distribution due to frictional heat source at the tool-chip interface, International Journal of Mechanical Sciences 43 (2001) 57-88.